Scientific
Research
Publishing

Measurement of Shear Stress Acting on Flat Plate Using Oil Film Interferometry

Takamitsu Fujino[1*], Masaki Endo[2], Hiromasa Suzuki[3], Yoko Sakakibara[4]

[1]Mechanical Engineering, Tokyo Denki University, Saitama, Japan
[2]Division of Mechanical Engineering, Tokyo Denki University, Saitama, Japan
[3]Production Systems Engineering Course, Tokyo Metropolitan College of Industrial Technology, Tokyo, Japan
[4]Division of Mechanical Engineering, Tokyo Denki University, Saitama, Japan
Email: *22rmm17@ms.dendai.ac.jp

Abstract

Measurements of frictional resistance play an important role in engineering practice. There are several types of air resistance acting on an aircraft, for example. One of them, frictional resistance, accounts for half of the air resistance. Oil film interferometry is one of methods for measuring the frictional resistance. Oil dropped on an object is thinly stretched by the frictional resistance. The bright and dark fringe pattern is generated when monochromatic light is applied to the oil film. The gradient of the oil thickness decreases with the lapse of time, and thus the spacing between neighboring the dark lines increases. The rate at which the spacing increases is proportional to the frictional resistance. In this study, the frictional resistance acting on a small area on a plate was measured and compared with the theoretical value. As a result, these results qualitatively agree well with each other.

Keywords

Oil Film Interferometry, Fluid Friction, Turbulent Flow, Interference Fringes

1. Introduction

Aircrafts, ships, and automobiles are required to conserve energy and to use effectively energy in order to reduce the use of fossil fuels. To promote energy conservation, it is necessary to reduce resistance, which can result in energy loss. In these vehicles, surface friction resistance has a significant impact, especially in aircraft, where surface friction resistance accounts for about 50% of the total resistance (Nakahashi, 2007) [1]. Therefore, even a small reduction in surface friction resistance can have a large effect on the energy conservation. Therefore, a

highly accurate measurement method of surface friction resistance is needed.

Since surface frictional resistance causes shear stress on the surface of objective body, surface frictional resistance can be determined by measuring the shear stress acting on the body surface. The measurement method for working on a flat plate surface has been studied for more than 20 years. However, a database to discuss the universality of the method has not yet been established.

Oil film interferometry is one of the methods to measure surface friction resistance. It is a measurement method proposed by Tanner and Blows. The advantage of this method is that the experimental apparatus is simple, and research is being conducted to put it to use in engineering practice. Henry *et al.* concluded that the oil film interferometry can be applied at high Reynolds numbers, but that its reproducibility must be verified by using oils of various nominal viscosities (H. C. H. Ng *et al.* 2007) [2].

In this study, we use the oil film interferometry to measure the shear stress on a flat plate in a flow field parallel to the flat plate, summarize the relation between the Reynolds number and the coefficient of surface friction resistance, and compare the results with theoretical values to confirm validity of the oil film interferometry.

2. Methodology

The oil film interferometry is one of methods of measuring local shear stress. When a wedge-shaped oil film is irradiated with monochromatic light, the bright and dark fringe pattern is observed due to optical path differences. A very small drop of oil is dropped onto a flat plate, and the shear stress acting on the oil by the air flow causes the oil to spread and the spacing between neighboring the dark lines to widen gradually. The shear stress is calculated from the speed at which the dark lines move. **Figure 1** illustrates the optical path difference of light in the thin oil film. Bright lines and dark lines appear alternately due to interference between light reflected from the surface of the oil and that from the contact surface between the oil and the flat plate. If the surface of oil film in contact with the air is extremely flat, the bright and dark fringe pattern is normal to the direction of the shear stress and the spacings between neighboring dark lines are equal to each other. **Figure 2** shows a schematic of the bright and dark fringe pattern generated in the oil. The thickness of the oil at the k-th dark line counted from the apex of the oil-film wedge, h_k, is given by the following equation,

$$h_k = \left(k + \frac{1}{2}\right)\lambda_0 \bigg/ 2\sqrt{n_{oil}^2 - n_{air}^2 \sin^2 \alpha} \quad (k = 0, 1, 2, \cdots)$$

and thus, the difference between the thicknesses of the oil film on the adjacent dark lines Δh is

$$\Delta h = \lambda_0 \bigg/ 2\sqrt{n_{oil}^2 - \sin^2 \alpha} \tag{1}$$

where λ_0, n_{oil}, and α are the wavelength of a light source, the refractive index of the oil, and the incident angle of the light, respectively. The sodium lamp is used
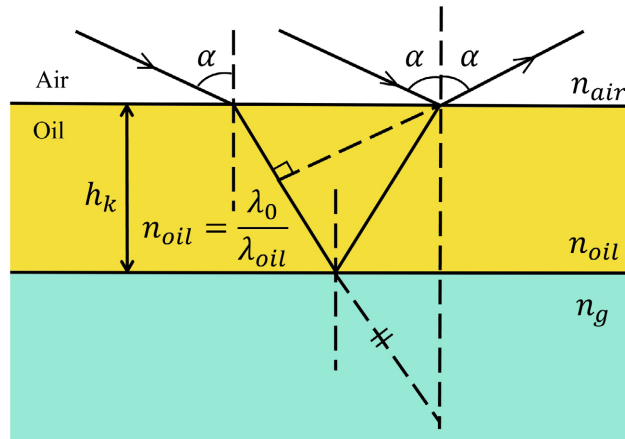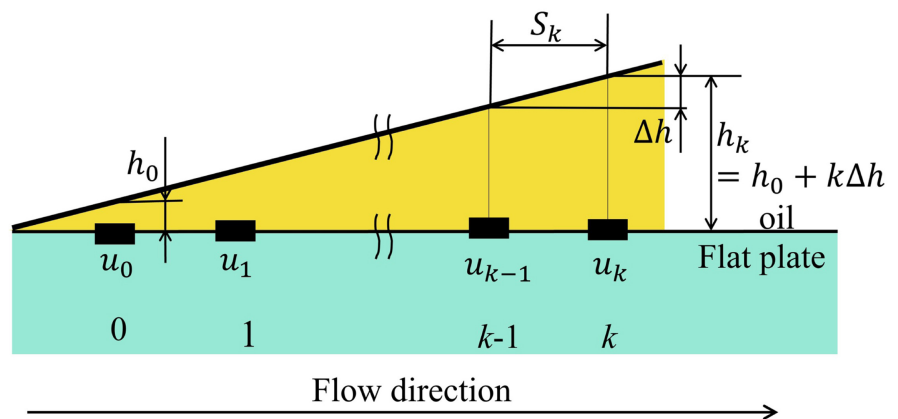
Figure 1. Optical path.

Figure 2. The bright and dark fringe pattern of oil.

as a light source for the interference.

The wedge-shaped film of oil on a flat plate gradually spreads downstream due to shear stress τ acting by the air, and the apex angle of the wedge becomes smaller. Assuming the oil is a Newtonian fluid, the velocity u_k of the oil at the k-th dark line can be expressed by the following equation.

$$u_k = \frac{\tau}{\mu} h_k = \frac{\tau}{\rho v} h_k \tag{2}$$

where τ, ρ, and v are the shear stress, the oil density, and the kinematic viscosity coefficient, respectively. Assuming that the shear stress τ does not vary locally, the spacing between neighboring dark lines, *i.e.*, the wavelength of the bright and dark fringe pattern S_k can be expressed by the following equation using Equation (2), because the difference in velocity between neighboring dark lines is proportional to the decrease in the wedge apex angle (Tsuji, Y. *et al.* 2021) [3].

$$\frac{dS_k}{dt} = u_k - u_{k-1} = \frac{\tau}{\mu}\left(h_k - h_{k-1}\right) = \frac{\tau}{\mu}\Delta h \tag{3}$$

Substituting Equation (1) into Equation (3) and solving for shear stress τ yields the following equation.

$$\tau = \frac{2\rho v \sqrt{n_{oil}^2 - \sin^2 \alpha}}{\lambda_0} \cdot \frac{\mathrm{d}S}{\mathrm{d}t} \tag{4}$$

From Equation (4), the shear stress τ can be obtained from the temporal variation of the fringe wavelength $\mathrm{d}S/\mathrm{d}t$.

3. Experimental Setup

A schematic view of the experimental apparatus is shown in **Figure 3**. The air supplied by the blower goes through the expansion section and passes through the rectifying grating, where the flow becomes uniform. The flow velocity is increased by reducing the cross-sectional area of the flow path in the compression section. A tripping wire is attached at the nozzle exit so that it forced the flow to become turbulent, and the turbulent boundary layer is formed on the flat plate. The flat plate was installed at the center of the nozzle exit in the height direction. The air velocity is changed by adjusting the input voltage of the blower with a variable autotransformer.

Figure 4 shows the optical system arrangement of the test section. As shown in **Figure 4(a)**, a very small drop of oil is applied to the test section, and it was illuminated with light from a sodium lamp. The camera is fixed on a tripod at $\alpha = 30°$ with respect to the vertical direction on the flat plate. The camera is set to a shutter speed of 1/200, an aperture value of F9, an ISO sensitivity of 250, and a pixel count of 4000×6000. The fringe pattern generated in the oil film was consecutively photographed for 500 s at 5-second intervals. Since the viscosity of the oil depends on the temperature of the oil (IIjima, H. *et al.* 2021) [4] (Kurita, M. *et al.* 2016) [5], the temperature of the oil was measured using a thermocouple under the assumption that the temperature of the oil is equal to that of the flat plate of the test section. As shown in **Figure 4(b)**, the flow velocity at the center of the nozzle exit was measured using a pitot tube and employed as the main stream velocity. The input voltage applied to the blower was varied in 10 V steps from 60 to 100 V using a variable autotransformer, and measurements were carried out three times at each input voltage.
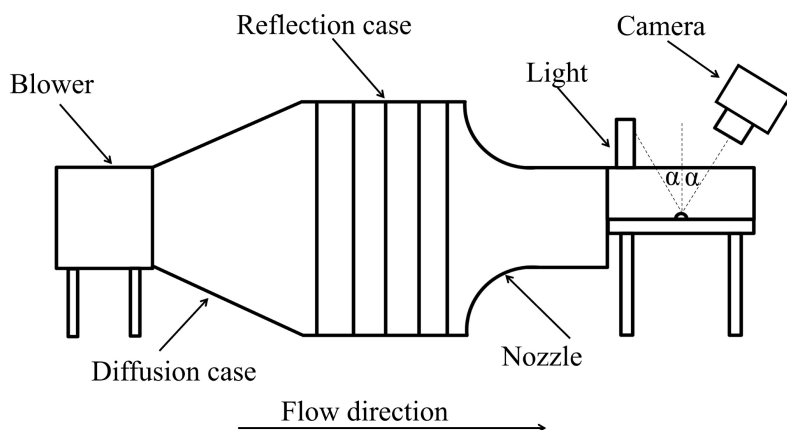

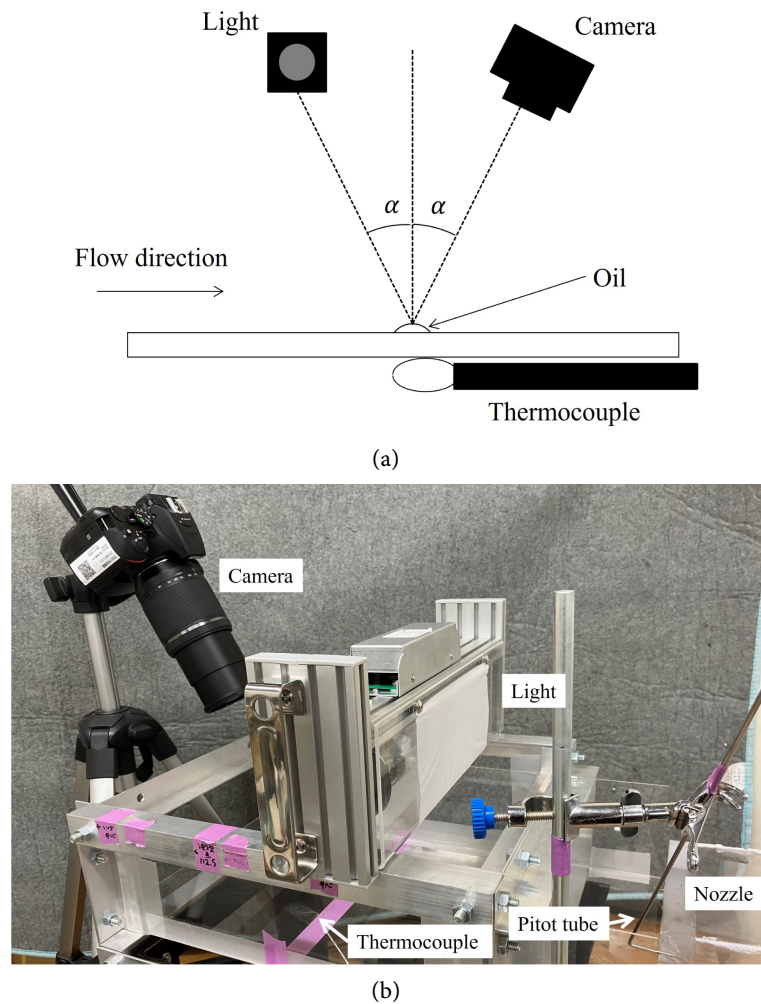**Figure 3.** Schematic view of experimental equipment.

(a)

(b)

Figure 4. Test section. (a) Schematic view; (b) Photo.

4. Results and Discussion

Figure 5 shows a binarized image of the bright and dark fringe pattern observed in the experiment. The air flows from the top to the bottom. **Figure 5(a)** is an image taken at 200 s after the start of photographing, and **Figure 5(b**) is an image at 500 s. Both images visualize the same region at a flow velocity of 14.3 m/s. The size of the image is a square with 4.2 mm (257 pixels) on a side. The oil is stretched by the shear stress caused by the air flow, and the oil thickness becomes thinner. As a result, the wavelength of the fringe pattern increases with time.

To estimate the typical fringe spacing between neighboring dark lines, FFT analysis was performed on 129 predetermined lines, which lie at an interval of two pixels, along the *x*-direction of the image shown in **Figure 5**. The dominant frequency components were determined, and the wavelength S was estimated for each line. The relation between the wavelength S of the fringe pattern and elapsed time t is shown in **Figure 6**. This shows the result of a line which lies at $y = 129$ pixels. In this figure, and the solid line is an approximately straight line
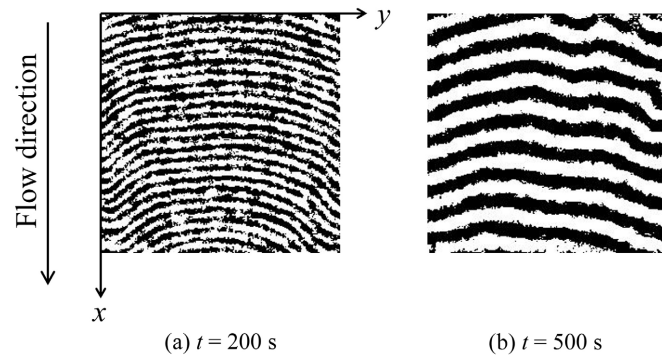
(a) t = 200 s   (b) t = 500 s
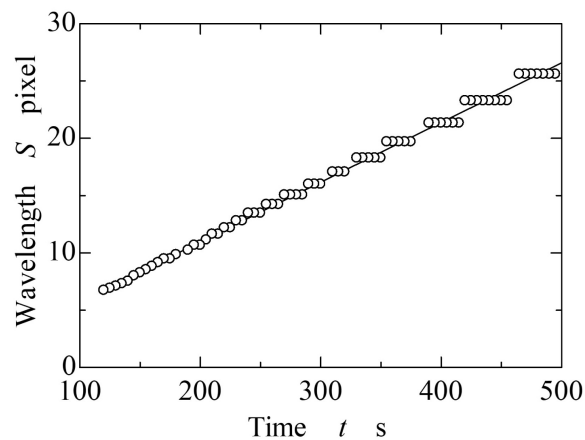
Figure 5. Binarized image.

Figure 6. Relation between wavelength and time.

obtained by the least square method. The wavelength S is proportional to the elapsed time t. The gradient dS/dt at each predetermined line was estimated. **Figure 7** shows the gradient dS/dt profile. The abscissa denotes the distance y from the left edge of the image. The values of dS/dt are scattered near both edges of the image.

Figure 8 shows variations of the average value ds/dt_A and the standard deviation σ of dS/dt with the number of continuous data n, which are selected so that a center position of the continuous data is located at a center of the image. Up to n = 100, the changes are very small in standard deviation σ and the gradient ds/dt. The average value of ds/dt is kept constant between n = 53 and 101, and the value of the standard deviation is mostly constant between n = 77 and 97. Thus, the number of continuous data n is determined to be 97.

In the same way, the average of dS/dt at the different flow velocities was calculated. **Figure 9** shows variation of dS/dt with Reynolds number. As the Reynolds number Re_x increases, dS/dt tends to increase. The shear stress was obtained by substituting the value of dS/dt into Equation (4). In this study, the values of ρ, n_{oil}, α, and λ_0 are constants. **Figure 10** shows variation of the coefficient of frictional resistance C_f with the Reynolds number. The circle marks denote the experimental results, where the shear stress τ is divided by the dynamic
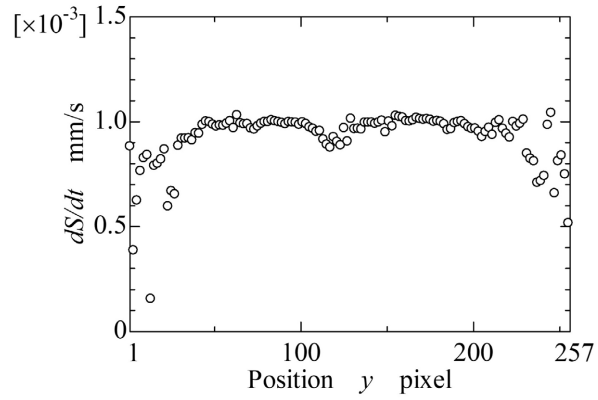
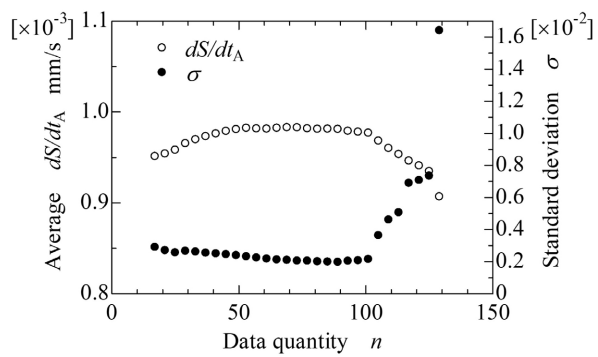**Figure 7.** Variation of dS/dt with position in y direction.

Figure 8. Variations of the average value ds/dt_A and the standard deviation σ of dS/dt with the number of continuous data n.
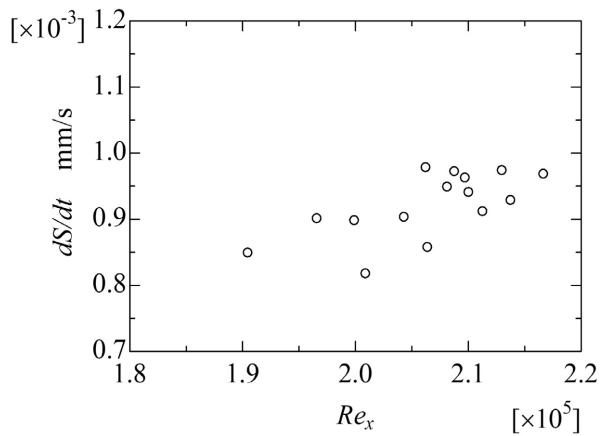

Figure 9. Variation of dS/dt with Re_x.

pressure of the mainstream. The solid line denotes the theoretical value of the local frictional resistance coefficient in turbulent flow given by White.

$$C_f = 0.026 Rex^{-1/7} \tag{5}$$

Equation (5) was derived as one of theoretical approximate expression using Coles' law of the wake under the assumption that the pressure gradient of main
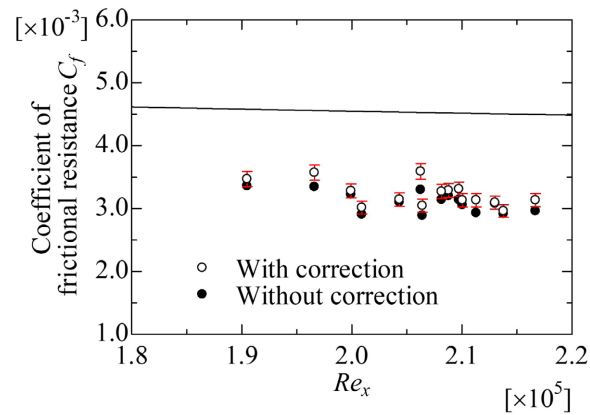
Figure 10. Friction resistance coefficient measured by OFI.

stream direction $dp/dx \approx 0$(D. Coles, 1956) [6], (D. Coles, 1968) [7]. This equation is known to include an error of plus or minus 2%. The coefficient of frictional resistance C_f by Equation (5) tends to decrease slightly with an increase in Reynolds number. The experimental results have the same tendency. The empty circle denotes the experimental result using the kinematic viscosity coefficient based on the atmospheric temperature and the solid circle denotes that based on temperature of the flat plate, onto which the oil is dropped. These results include an error of plus or minus 3.5% in the value due to the camera installation angle, temperature measurement, and manometer error. In the empty circles, the error is shown by the error bar. Furthermore, the value of dS/dt deviates by about 5% depending on how long the time is used to estimate the value of dS/dt. The temperature correction increased the coefficient of friction resistance C_f and brought it closer to the theoretical value. The temperature correction improved the accuracy by up to 7%.

5. Conclusions

The oil film interferometry was used to measure the shear stress from the flow field parallel to the flat plate. A very small drop of oil was dropped onto the flat plate, and the shear stress was calculated under the assumption that the shear stress does not change locally and the surface of the oil in contact with the air is extremely flat. Comparing the obtained results with the theoretical value, the following conclusions were drawn.

- The local coefficient of frictional resistance C_f slightly decreases with increasing the Reynolds number, which is the same tendency as White's equation.

- The temperature correction leads to an improvement in accuracy.

The oil film interferometry with a very small drop of oil is useful for the measurement of the local shear stress. The bright and dark fringe pattern observed by the interferometry is normal to the direction of the shear stress. Analysis utilizing this characteristic may help reveal the local direction of the shear stress in the future. We expect great progress in analyzing the wall flow from using this

method.

Conflicts of Interest

The authors declare no conflicts of interest regarding the publication of this paper.

References

[1] Nakahashi, K. (2007) Aircraft Aerodynamics and Optimization. *Journal of Nagare*, **26**, 259-265.

[2] Ng, H.C.H., Marusic, I., Monty, J.P., Hutchins, N. and Chong, M.S. (2007) Oil Film Interferometry in High Reynolds Number Turbulent Boundary Layers. *Proceedings of the* 16*th Australasian Fluid Mechanics Conference*, Gold Coast, Australia, 2-7 December 2007, 807-814.

[3] Tsuji, Y., Ido, A. and Nishioka, M. (2021) Universality of Mean Velocity Profile in High Re-Number Turbulent Boundary Layer. *Transactions of the JSME*, **87**, 1-24. (In Japanese) https://doi.org/10.1299/transjsme.21-00280

[4] Iijima, H., Uchiyama, T. and Kato, H. (2021) Measurement of Skin Friction Distribution Using Oil Film for Industrial Wind Tunnels. *Transactions of the Visualization and Information Society of Japan*, **41**, 28-34. https://doi.org/10.3154/tvsj.41.28

[5] Kurita, M. and Iijima, H. (2016) Oil-Film Interferometry Using Correction for Variation of Oil-Viscosity with Temperature. *Proceedings of the* 48*th Fluid Dynamics Conference*/*the* 34*th Aerospace Numerical Simulation Symposium*, Kanazawa, 6-8 July 2016, 207-211.

[6] Coles, D. (1956) The Law of the Wake in the Turbulent Boundary Layer. *Journal of Fluid Mechanics*, **1**, 191-226. https://doi.org/10.1017/S0022112056000135

[7] Coles, D. (1968) The Young Person's Guide to the Data. In: Coles, D.E., Hirst, E.A., Eds., *AFOSR-IFP Stanford Conference on Computation of Turbulent Boundary Layers*, *Thermosciences Division*, Stanford University, Calphonia, 1-45.